processes

Article

Physical Simulation Experiments of Hydraulic Fracture Initiation and Propagation under the Influence of Deep Shale Natural Fractures

Zhou Hu [1], Pengfei Chen [2], Wei Jiang [1], Yadong Yang [1], Yizhen Li [1], Longqing Zou [1], Huaming Wang [1], Yuping Sun [3,*] and Yu Peng [4,*]

[1] Shale Gas Exploration and Development Department, CNPC Chuanqing Drilling Engineering Co., Ltd., Chengdu 610051, China
[2] Research Institute of Natural Gas Technology, PetroChina Southwest Oil and Gas Field Company, Chengdu 610213, China
[3] PetroChina Research Institute of Petroleum Exploration & Development, Beijing 100083, China
[4] State Key Laboratory of Oil and Gas Reservoir Geology and Exploitation, Southwest Petroleum University, Chengdu 610500, China
* Correspondence: sunyuping01@petrochina.com.cn (Y.S.); pengyu_frac@foxmail.com (Y.P.)

Abstract: Horizontal wells' multi-section and multi-cluster hydraulic fracturing plays an important role in the efficient development of shale gas. However, the influence of the perforating hole and natural fracture dip angle on the process of hydraulic fracture initiation and propagation has been ignored in the current researches. This paper presents the results related to a tri-axial large-scale hydraulic fracturing experiment under different natural fracture parameters. We discuss the experimental results relating to the near-wellbore tortuosity propagation of hydraulic fractures. Experimental results showed that the triaxial principal stress of the experimental sample was deflected by the natural fracture, which caused significant near-wellbore tortuosity propagation of the hydraulic fractures. The fractures in most rock samples were not perpendicular to the minimum horizontal principal stress after the experiment. As well, the deflection degree of triaxial principal stress direction and the probability of hydraulic fractures near-wellbore tortuosity propagation decreased with the increase of the natural fracture dip angle. After hydraulic fractures' tortuous propagation, the hydraulic fractures will propagate in the direction controlled by the triaxial stress in the far-wellbore area. For reservoirs with natural fractures, proppant in hydraulic fracturing should be added after the fractures are fully expanded to prevent sand plugging in tortuous fractures. When the permeability of natural fractures is low, the volume of fracturing fluid entering natural fractures is small, and hydraulic fractures are easy to pass through the natural fractures.

Keywords: shale gas; hydraulic fracturing; fracture dip angle; near wellbore distortion; fracture permeability

Citation: Hu, Z.; Chen, P.; Jiang, W.; Yang, Y.; Li, Y.; Zou, L.; Wang, H.; Sun, Y.; Peng, Y. Physical Simulation Experiments of Hydraulic Fracture Initiation and Propagation under the Influence of Deep Shale Natural Fractures. *Processes* **2023**, *11*, 1934. https://doi.org/10.3390/pr11071934

Academic Editor: Carlos Sierra Fernández

Received: 6 June 2023
Revised: 25 June 2023
Accepted: 26 June 2023
Published: 27 June 2023

1. Introduction

Shale reservoirs have extremely low porosity and permeability, which can be obviously impacted by mineral deposition [1]. In the development of shale gas, hydraulic fracturing plays an important role in connecting the wellbore and reservoir matrix, establishing the gas flow path, and reducing gas seepage resistance [2]. The hydraulic fracture influences the whole life of the shale gas well, including the fracturing period, shut-in period, and production [3]. Numerical simulation is the main means of studying the impact of hydraulic fractures on reservoir fluid flow and production [4], especially in the production of shale gas reservoirs [5]. However, the propagation law of hydraulic fractures is difficult to obtain through numerical simulation and needs to be studied through fracturing experiments [6]. The interaction between hydraulic fractures and natural fractures has been widely studied, which directly determines the complexity of the fracture network, the invasion range of fracturing fluid, and the stimulation effect of shale gas wells [7]. The complexity of the fracture network deeply impacts the production of a shale gas well [8]. As an important fracture parameter, the influence of natural fracture dip angle on the propagation of hydraulic fractures is rarely discussed [9]. As well, the fracture initiation and fracture propagation patterns near the horizontal wellbore, which seriously impact the near-wellbore friction during fracturing and the tortuosity and resistance of shale gas flow during production, have always been regarded as the research focus of hydraulic fracturing. Therefore, the analysis of fracture propagation patterns and influencing factors in the near wellbore area is of great significance for improving the effectiveness of fracturing construction.

Natural fractures are widely distributed in shale reservoirs. Due to the low porosity and permeability of the shale matrix, effective activation or connection of natural fractures has become an important way to improve the production of shale gas wells. Building a fracture network has become the main goal of current fracturing construction. Therefore, the study of the influence of natural fractures on the propagation of hydraulic fractures is of great significance. Many researchers discussed the intersection mechanism of hydraulic fracture and natural fracture through laboratory experiments [10]. Lamont et al. [11] and Daneshy et al. [12] used outcrop rock samples as experimental samples for the first time to conduct fracturing experiments and discussed the influence of natural fractures on hydraulic fracture propagation. Their research shows that the scale of natural fractures has a significant impact on the expansion of hydraulic fractures. Real triaxial large-scale physical simulation experiments were carried out using natural shale outcrop rock samples and artificial gypsum rock samples. As well, the impact of the intersection angle and horizontal principal stress difference on the hydraulic fracture passing through the naturally weak surface was discussed. [13–15]. As well, the influence of natural fracture shear strength on fracture intersection criterion is discussed by fracturing experiment [16,17]. Natural fractures and formation stress control the geometry and propagation behavior of hydraulic fractures [18]. Gu et al. verified the intersection criterion between hydraulic fractures and natural fractures through experiments [19]. This shows that natural fractures are of great significance to the construction of complex fracture networks. As well, complex fracture network is conducive to the efficient development of Shale gas [20]. The influence of the angle between natural fractures and hydraulic fractures on fracture propagation and the intersection criterion between hydraulic fractures and natural fractures is mainly discussed. However, hydraulic fractures in the horizontal well of the shale reservoir may have the same angle as natural fractures with different dip angles. Therefore, the influence of natural fracture inclination on hydraulic fracture propagation is worth studying. Fatahi et al. [21] discussed the interaction between hydraulic fractures and natural fractures through hydraulic fracturing experimental research and numerical simulation methods. The research shows that the smaller the angle between the natural fracture and the minimum horizontal principal stress, the easier the hydraulic fracture will pass through the natural fracture. The influence of bedding on fracture propagation in coal was also discussed through experiments and numerical simulation [22]. Based on these studies, the optimization scheme of hydraulic fracturing operation is also proposed [23]. Zou et al. [24] use CT scanning technology to analyze the hydraulic fracture geometry of shale rock samples with natural fractures after a fracturing experiment. The shear slip characteristics of natural fractures during hydraulic fracturing were analyzed through experiments [25]. The hydraulic fracture approach angle will affect the shear slip degree of natural fractures [26]. The vertical propagation mechanism of hydraulic fracture is analyzed by fracturing experiments with samples containing interlayers and bedding [27]. The influence of bedding and natural fractures on hydraulic crack propagation has also been confirmed through numerical simulation [20]. Above all, the impact of shale bedding on fracture height and the interaction between hydraulic fractures and natural fractures are considered in a large-scale hydraulic fracturing physical simulation experiment. A large number of studies show that natural fractures significantly affect the expansion of hydraulic fractures [28,29]. As well, many intersection mechanism models between hydraulic fractures and natural fractures have been proposed [30]. However, few studies have discussed the influence of fracture dip angle on hydraulic fracture propagation with complex natural fracture networks and hydraulic fractures with near-wellbore tortuosity propagation. The migration of proppant in fractures is affected by the near-wellbore tortuosity propagation of hydraulic fractures. This is because curved fractures increase the migration resistance of proppant in the fracturing fluid, which can easily cause proppant to accumulate at the fracture opening and block the flow channel. This situation will seriously impact fracture propagation and hinder the construction of the fracture network. Therefore, the study of hydraulic fractures' near-wellbore tortuosity propagation is of great significance.

In this paper, cement samples with natural fractures were used to study the influence of natural fracture dip angle on hydraulic fracture initiation and propagation through a tri-axial large-scale hydraulic fracturing experiment. The influence of natural fracture dip on the near-wellbore triaxial principal stress and hydraulic fractures' near-wellbore tortuosity propagation was discussed. As well, the influence of horizontal principal stress differences on the propagation of hydraulic fractures and the intersection of hydraulic fractures and natural fractures is analyzed.

2. Materials and Methods

2.1. Experimental Equipment and Sample

The real tri-axial large-scale hydraulic fracturing initiation and propagation physical simulation system (Figure 1) is composed of a triaxial stress loading chamber, a liquid pumping system, a pneumatic control system, and a digital control system. There is a hydraulic jack in the X-Y-Z direction in the triaxial stress loading chamber, which can provide compressive stress to simulate the triaxial principal stress in the formation. One of the hydraulic jacks is installed at the bottom of the loading chamber to apply vertical stress to the experimental sample. The other two are installed in a horizontal direction to apply two mutually perpendicular horizontal stresses to the experimental sample. Set stress values in three directions in the experimental system, and the experimental equipment will load corresponding stresses in the three directions to meet the experimental conditions.

Figure 1. The real tri-axial large-scale hydraulic fracturing initiation and propagation physical simulation system.

A liquid pumping system, which is connected to an artificial wellbore in the cement sample, can provide constant pressure pumping and constant displacement pumping. The pump rate range is from 1 mL/min to 120 mL/min. The pump pressure range is from 0 MPa to 100 MPa. The maximum volume of the liquid injection pump is 500 mL. The pipeline and wellbore should have strong pressure-bearing capacity to meet the requirements of the fracturing experiment. During the experiment, the liquid is pumped into the intermediate container, and the dyed liquid, which is used to simulate fracturing fluid, is injected into the artificial wellbore by the intermediate container. Throughout the entire experiment, the pump pressure of the liquid will be recorded until the end of the experiment.

Experimental samples are formed by cement and sand in the mold (Figure 2b). An artificial wellbore, which is a steel pipe with an external thread for enhancing the friction between the wellbore and sample, is inserted into the mold during the cement setting. It should be noted that the steel pipe did not fully fill the wellbore of the experimental sample. In the experiment described in this paper, the wellbore of the rock sample is 5 mm longer than the steel pipe, which allows the hydraulic fractures to propagate from the bottom of the well after the fracturing experiment, and the effect is comparable to the perforation process in actual construction. The experimental samples were cut by a water jet with reference to different natural fracture dip angles (Table 1) and recombined with cement. For each rock sample, we used the same material for bonding to ensure that the natural fracture permeability in each rock sample tends to be consistent. This can effectively avoid the impact of large differences in natural fracture permeability on the fracturing experimental results.

(**a**) casing pipe

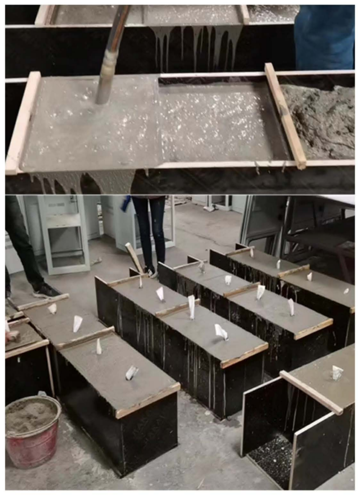

(**b**) Cement sample preparation

(**c**) Cutting sample to build natural fractures

Figure 2. Experimental sample preparation.

Table 1. Experimental scheme.

Sample No	Sizes of Rock Sample (mm)	Depth of the Wellbore (mm)	Length of Steel Pipe (mm)	Inner Diameter of Steel Pipe (mm)	Triaxial Principal Stress X-Y-Z (MPa)	Number of Natural Fracture	Natural Fracture Dip Angle (°)
P1-1	300 × 300 × 300	150	145	25	50-60-60	1	80
P1-2					50-65-65	1	80
P1-3					50-70-70	1	80
P2-1					50-60-60	1	60
P2-2					50-65-65	1	60
P2-3					50-70-70	1	60
P3-1					50-60-60	1	40
P3-2					50-65-65	1	40
P3-3					50-70-70	1	40
P4					50-65-65	2	80/80
P5					50-65-65	2	80/−80
P6					50-65-65	2	40/40
P7					50-65-65	2	40/−40
P8					50-65-65	2	80/0

2.2. Experimental Method and Procedure

Experimental research is the main means to explore the propagation of hydraulic fractures and the interaction criteria between hydraulic fractures and natural fractures. The experimental methods and steps in this paper are as follows.

(1) Polish the irregular residue on the sample surface to make the surface of the samples regular and flat. The installation process of the rock sample can be performed smoothly.
(2) Put the experimental sample into the predetermined position of the triaxial stress loading chamber through the lifting machine. Then install metal cushion blocks between the hydraulic pump and rock sample to make it fully fit with the surface of the sample and ensure uniform stress on the sample.
(3) Add the pre-configured fracturing fluid, which is prepared with glycerin and dye, into the fracturing intermediate container. Then connect the fracturing fluid pipeline outlet with the pressure sensor, and then connect the pipeline with the upper part of the wellbore.
(4) Apply triaxial stress to the rock sample by using the hydraulic pump. In this process, it is necessary to maintain the slow and synchronous loading of three-dimensional stress.
(5) After the triaxial stress of the rock sample reaches the predetermined value, pump fluid into the sample at a small pumping rate to fill the fracturing fluid injection pipeline and wellbore space. When the pipeline pressure has an upward trend, inject fracturing fluid into the wellbore with a pre-designed pumping rate, and record the changes in pumping pressure and pumping rate during fracturing through the data acquisition system. When the pressure curve of the computer acquisition system window shows a sudden drop in pressure, it indicates that the sample has successfully fractured. Then continue to record the change rule of injection pressure with injection displacement.
(6) Stop the pump to complete the test when the predetermined pumping volume is reached. Then remove the sample from the triaxial stress loading chamber with a lifting machine. Use a large cutting machine to cut the sample along the fracture surface, observe and record the space coordinate position of the residual tracer trace from the cutting surface, and determine the shape and extension direction of the crack initiation.

To discuss the influence of natural fracture dip and horizontal stress difference on fracture propagation, each group of experiments was set with the same rock sample size, wellbore depth, and steel pipe size, only changing the three-dimensional principal stress, the number of fractures, and natural fracture dip. The experimental design scheme was shown in Table 1. The natural fracture of each experimental sample was shown in Figure 3. The pump rate is set to 30 mL/min in the fracturing experiment. Although temperature changes can impact the structure of shale [31], the fracturing construction time is relatively short, so the influence of temperature on crack propagation was ignored in the experimental design of our work.

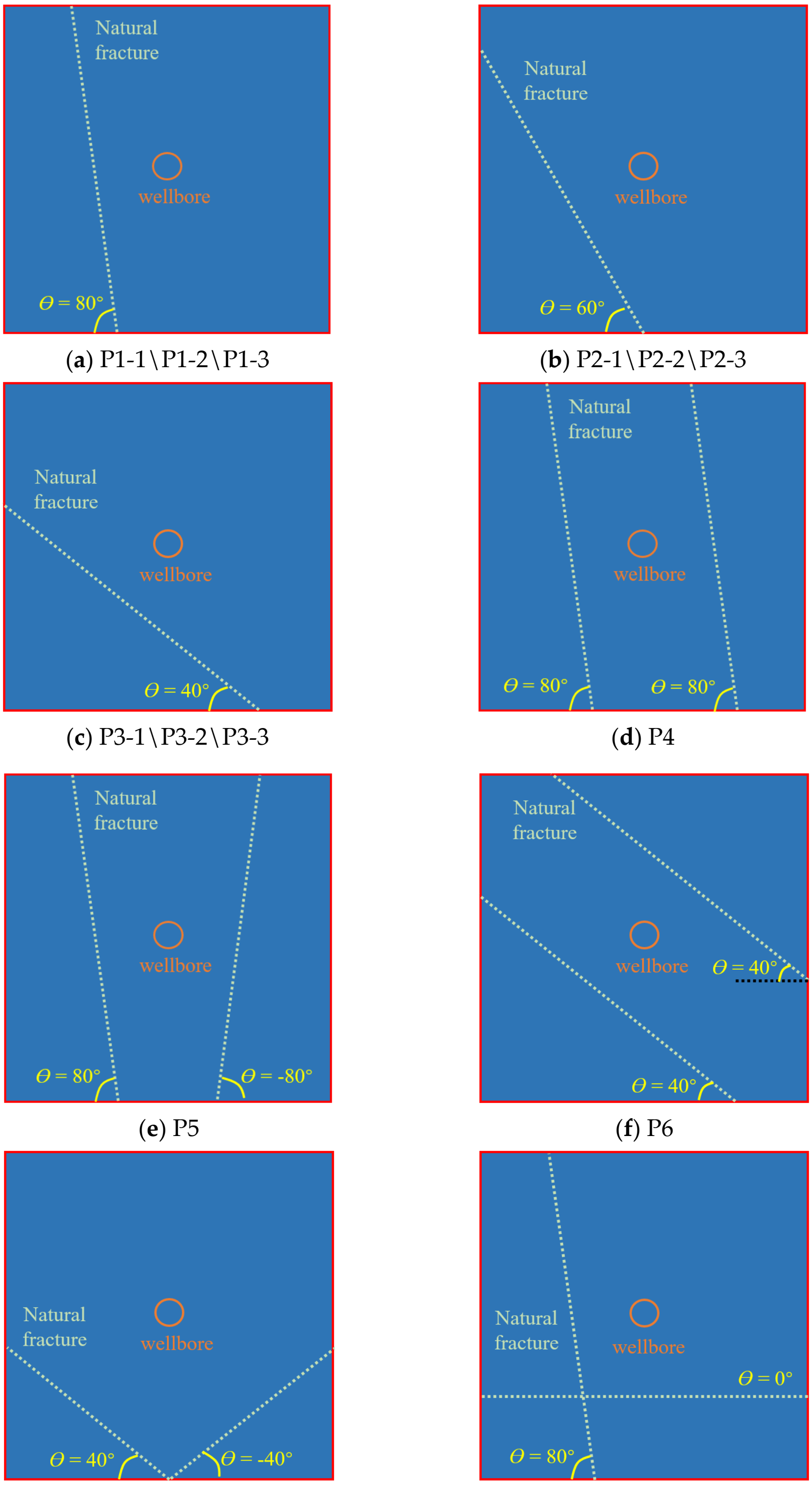

(**a**) P1-1\P1-2\P1-3 (**b**) P2-1\P2-2\P2-3
(**c**) P3-1\P3-2\P3-3 (**d**) P4
(**e**) P5 (**f**) P6
(**g**) P7 (**h**) P8

Figure 3. Schematic diagram of experimental sample and natural fracture (the view is wellbore direction).

3. Results and Discussion

The sample was broken by physical tools after the hydraulic experiment. The morphology of hydraulic fractures in rock samples is recorded (Figure 4). Due to the staining of the fracturing fluid, the hydraulic fracture morphology in the rock sample after the fracturing experiment and the intrusion of the fracturing fluid into the natural fractures can be clearly distinguished. As well, the fractures in the sample were redrawn with the drawing software (Figure 5). Based on the redrawn fracture morphology, the propagation mechanism of hydraulic fractures can be analyzed. As well, the influence of natural fracture dip on fracture propagation is discussed.

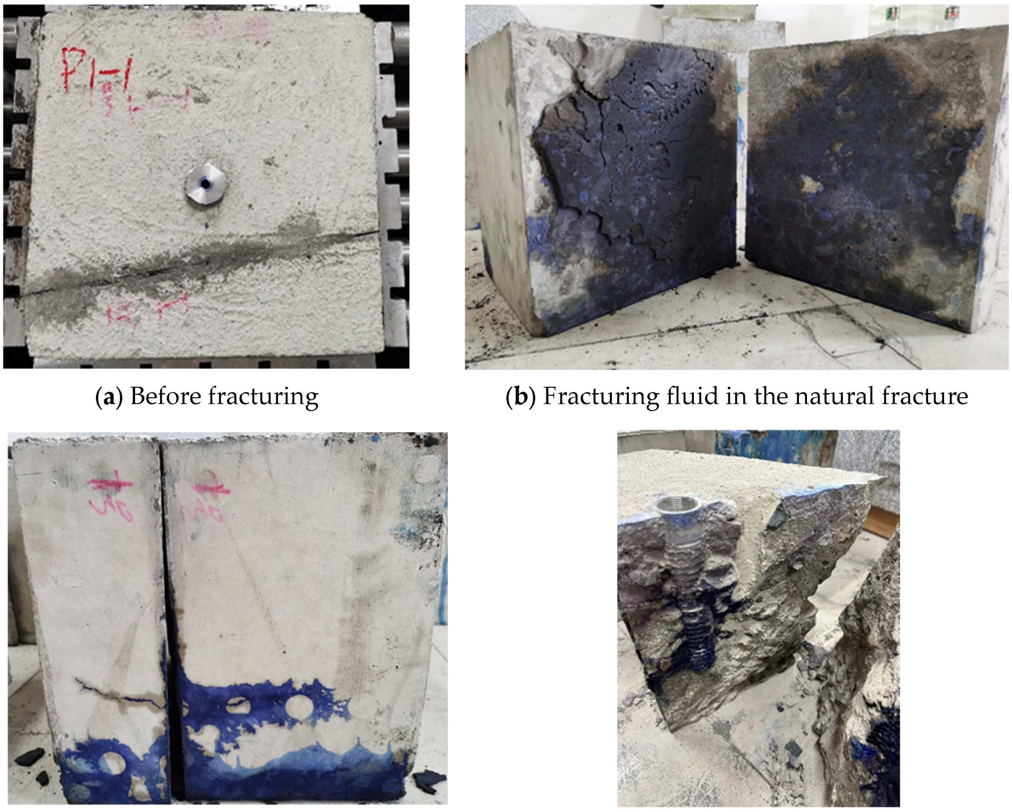

(**a**) Before fracturing (**b**) Fracturing fluid in the natural fracture

(**c**) Hydraulic fracture penetrating sample (**d**) Hydraulic fracture in sample

Figure 4. Experimental sample after fracturing.

From the hydraulic fracture morphology of the above 14 sets of experiments, it is obvious that hydraulic fractures do not pass through natural fractures in most cases. When the inclination angle of natural fractures is 80°, hydraulic fractures all pass through natural fractures, such as P1-1, P1-2, P1-3, P4, and P5. When the inclination angle of the natural fracture is 60°, only the hydraulic fractures in the case of P2-1 pass through the natural fracture. This result is in line with many current studies on the intersection of natural and hydraulic fractures, where the larger the inclination angle of natural fractures, the easier it is for them to pass through natural fractures [19]. However, there were many hydraulic fractures in the experimental results that were not perpendicular to the minimum horizontal principal stress set in the experiment. Tortuosity propagation of hydraulic fractures occurs in the near-wellbore area. This indicates that there is a difference between the horizontal principal stress and the pre-set principal stress during the experimental process. This is caused by natural crack-induced stress and perforation hole stress, and the smaller the inclination angle of the natural crack, the more the main stress is affected.

It is generally believed that the expansion of hydraulic fractures will be affected by the maximum and minimum horizontal principal stress. The initiation and propagation of hydraulic fractures are in the direction perpendicular to the minimum horizontal principal stress at the borehole. This phenomenon has also been confirmed in most large physical simulation experiments without prefabricated fractures [32]. Under the influence of perforation and induced stress of natural fracture near-wellbore in this experiment, the initiation and propagation mode of hydraulic fractures becomes very complex in our experiment. It shows a near-wellbore distortion effect that is not completely controlled by the maximum and minimum horizontal principal stress.

The hydraulic fracture morphology of shale is strongly influenced by natural fractures [33]. The fractures perpendicular to the wellbore in P1–2 do not intersect with the bottom of the well. First, the fractures parallel to the wellbore communicate with the natural fractures, forming a large leak-off, and then the fracture initiates and propagates from the natural fracture in the direction perpendicular to the wellbore. This phenomenon shows that the fracture distortion effect influenced by complex natural fractures is only effective in the near-wellbore position. After the fracture propagates far away from the stress concentration area, the fracture propagation is controlled by triaxial principal stress and conforms to the stress control theory. In the samples with only distorted fractures, such as P2-2, P2-3, P3-1, P3-3, P8, etc., the fractures may propagate according to the mode of crustal stress control after pumping for a period of time. When the natural fracture density of the reservoir is high, there will be a large number of fractures with various dip angles near the well. In this case, sand plugging is easy to form, and the amount of pre-fluid needs to be increased. After the fracture perpendicular to the direction of the minimum horizontal principal stress is fully expanded, a sand-adding operation can be carried out.

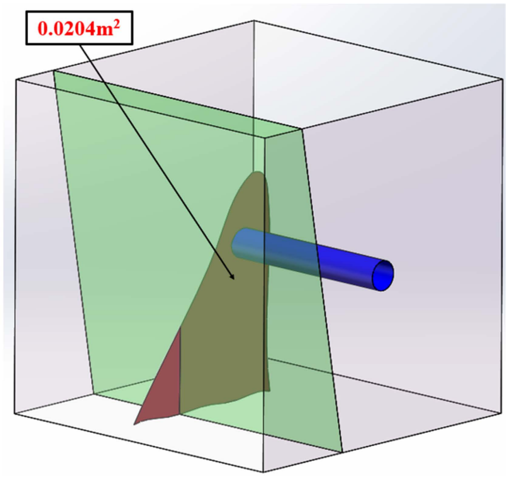

(**a**) P1-1

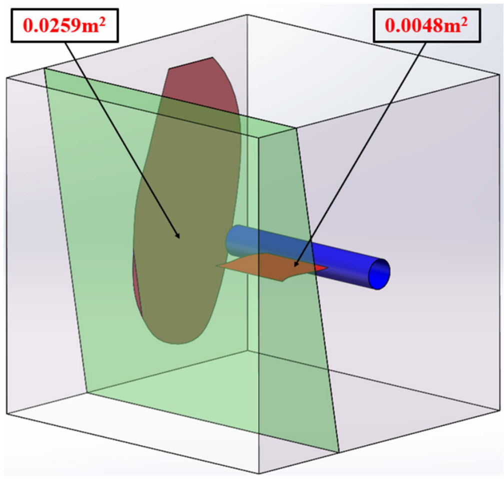

(**b**) P1-2

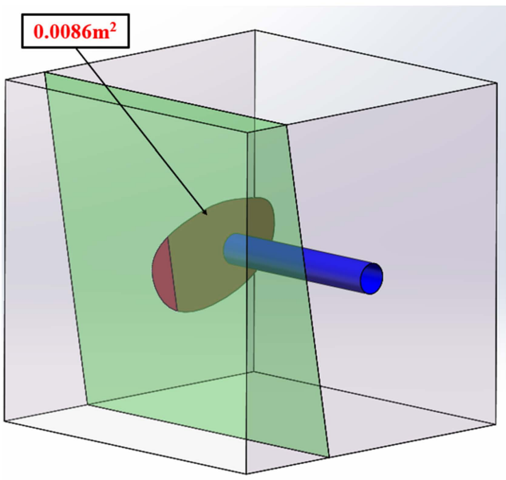

(**c**) P1-3

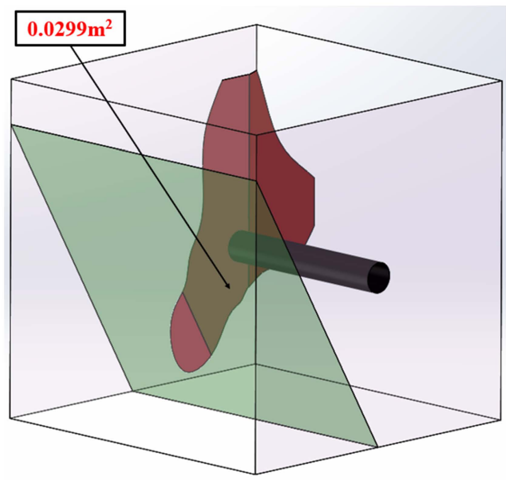

(**d**) P2-1

Figure 5. *Cont.*

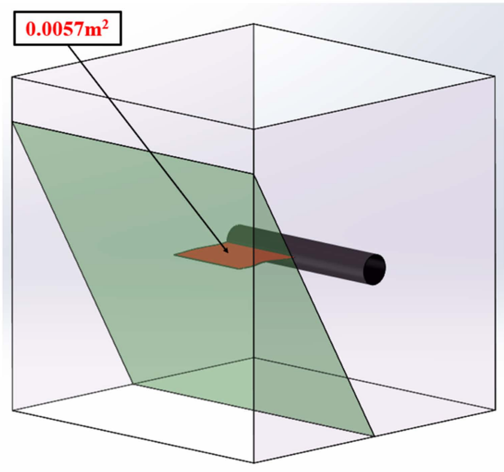

(**e**) P2-2

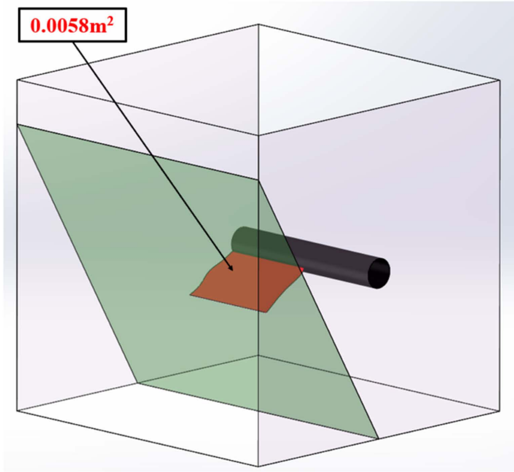

(**f**) P2-3

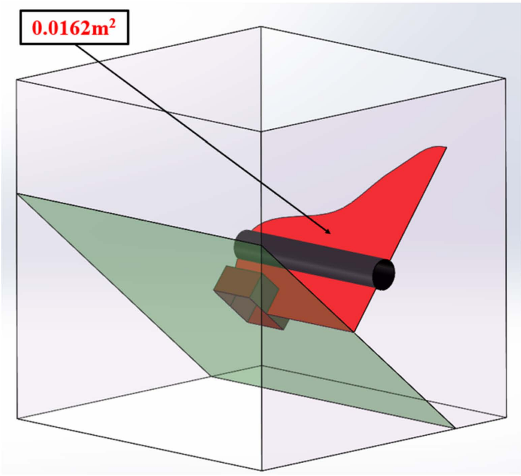

(**g**) P3-1

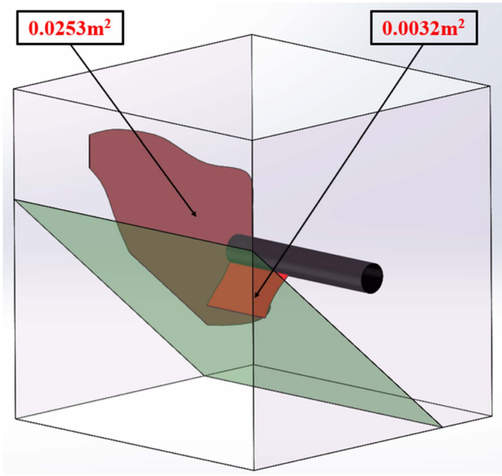

(**h**) P3-2

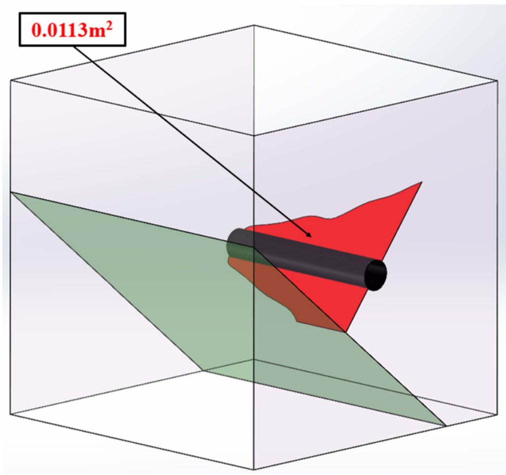

(**i**) P3-3

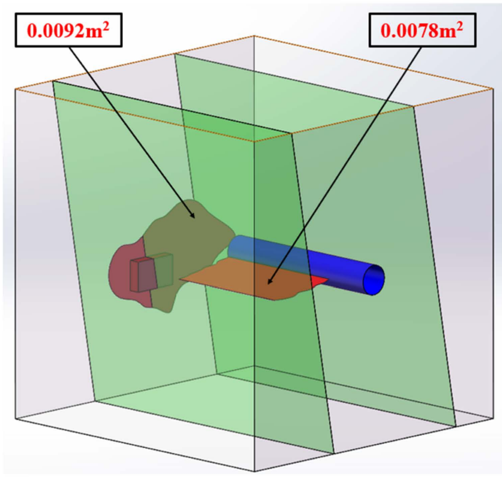

(**j**) P4

Figure 5. *Cont.*

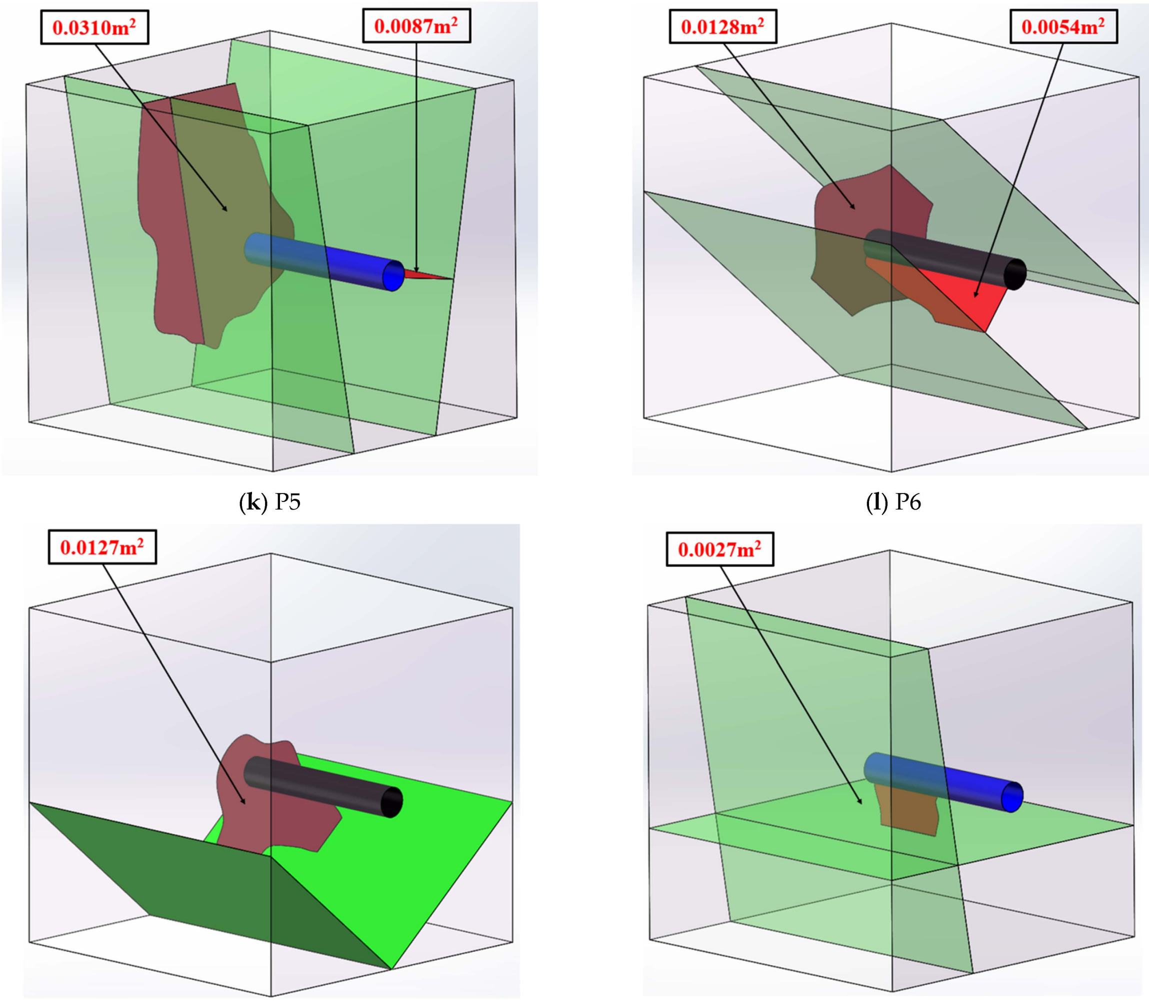

(**k**) P5 (**l**) P6

(**m**) P7 (**n**) P8

Figure 5. Fracture morphology after the experiment.

The permeability of hydraulic fractures has an extremely important impact on the expansion of fractures. According to previous experimental results, under the maximum and minimum horizontal principal stress differences (10, 15, and 20 MPa) set in this experiment, the artificial fractures should completely pass through the natural fractures. Under the experimental conditions in this paper, natural fractures are cemented and filled again by cement, but the leak-off volume of fracturing fluid will increase significantly after hydraulic fractures intersect with natural fractures. In the experimental results, only a few of the natural fractures in the sample are not completely colored. The massive fracturing fluid leak-off in natural fractures causes the artificial fractures to turn along the natural fractures instead of passing through the natural fractures. It has greatly increased our confidence in building artificial fracture networks in deep shale gas reservoirs.

When the natural fracture dip angle is greater than 80°, hydraulic fractures easily penetrate natural fractures, and the hydraulic fracture propagation direction is mainly in the direction of the vertical minimum horizontal principal stress [34,35], such as P1-1, P1-2, and P1-3. With the prefabricated natural fracture dip angle decreasing (from 80° to 60° and then to 40°), the deflection degree of the maximum and minimum horizontal principal stress directions increases. As well, the shape of the hydraulic fracture gradually deviates from the control of maximum and minimum horizontal principal stresses. When the natural fracture dip angle is 60°, the fractures parallel to the wellbore direction appear in experiments P2-2 and P2-3. When the natural fracture dip angle is 40°, the fractures parallel to the wellbore direction appear in the experiments of P3-1, P3-2, and P3-3.

The stress-sensitive effect of natural fractures impacts the permeability of natural fractures and the fracturing fluid leak-off in natural fractures. From the three groups of experiments (P1-1P1-3, P2-1P2-3, and P3-1P3-3), it can be analyzed that the leak-off volume of fracturing fluid in natural fractures gradually decreases with the increase of the difference between the maximum and minimum horizontal principal stresses, as shown in Figure 6. Especially when the difference between the horizontal principal stresses is more than 20 MPa, the spread of fracturing fluid in the natural fracture will be strongly inhibited, and only a part of the natural fracture area in the sample is stained. This is because it is difficult to open natural fractures, making it difficult for fracturing fluid to enter natural fractures under high stress. In the experiments of P4P8, the difference between the maximum and minimum horizontal principal stress is 15 MPa. As well, leak-off inhibition only occurs in the P6 sample. Therefore, in the fracturing construction of deep shale gas wells, the fracturing fluid leak-off in natural fractures may be inhibited when the maximum and minimum horizontal principal stress differences are greater than 20 MPa. This will impact the hydration fracture network and reduce the fracturing effect. The permeability of natural fractures and matrix can be enhanced by corrosion filler [36], which can promote the invasion of fracturing fluid in natural fractures and enhance the complexity of the fracture network. Therefore, the effect of stimulation can be improved by the corrosion of fracture-filling materials in fracturing construction.

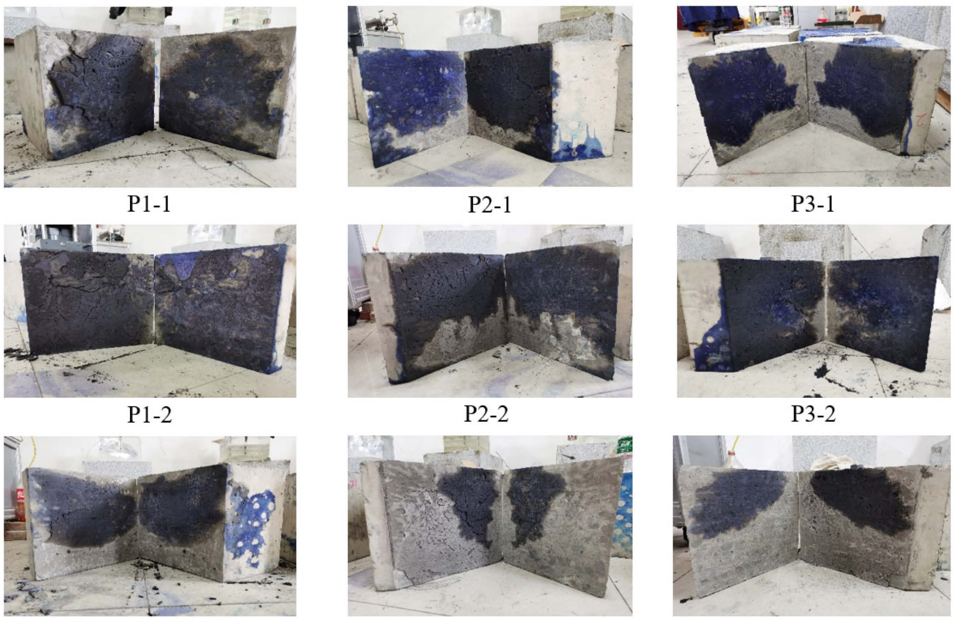

Figure 6. Fluid intrusion in natural fractures.

The experiments of P4–P8 show hydraulic fracture initiation and propagation under the influence of multiple groups of natural fractures. Comparing P4, P5, P6, and P7, it is shown that hydraulic fractures are easier to pass through high-dip-angle fractures near the wellbore. We assumed that the influence of a high dip angle fracture on horizontal principal stress is not obvious, and hydraulic fractures are easier to crack and expand in the non-dip mode. The experiments of P8 show that the maximum and minimum horizontal principal stresses are deflected by horizontal natural fractures and high-angle fractures. After the fracture initiated from the perforation hole, the horizontal fracture was directly communicated along the minimum horizontal principal stress. After the natural fracture was communicated, a large amount of leakage occurred, and the fracture almost no longer propagated to the rest.

4. Conclusions

In this work, 14 sets of fracturing experiments were completed by the real tri-axial large-scale hydraulic fracturing initiation and propagation physical simulation system. By observing the morphology of hydraulic and natural fractures in experimental rock samples, we redrew the fracture morphology through software. Through the analysis of experimental results, the influence of natural fracture dip on hydraulic fracture propagation is discussed. The influence of natural fracture permeability on the propagation of hydraulic fractures under different stress conditions is analyzed. This work also conducted an analysis and discussion on the influencing factors of near-wellbore distortion propagation.

(1) The direction of triaxial principal stress will be deflected by the near-wellbore natural fracture, which causes significant near-wellbore tortuosity propagation of hydraulic fractures. As well, the deflection degree of the triaxial principal stress direction and the probability of hydraulic fractures near-wellbore tortuosity propagation is negatively correlated with the natural fracture dip angle.
(2) The influence of high-dip angle fracture on the maximum and minimum horizontal principal stresses is not obvious. In this case, the propagation of hydraulic fracture is also controlled by the three-dimensional principal stress. With the prefabricated natural fracture dip angle decreasing (from 80° to 60° and then to 40°), the deflection degree of the maximum and minimum horizontal principal stress directions increases. As well, the shape of the hydraulic fracture gradually deviates from the control of maximum and minimum horizontal principal stresses.
(3) The hydraulic fractures will propagate in the direction controlled by triaxial stress in the far-wellbore area after tortuously propagating. For reservoirs with natural fractures, proppant in hydraulic fracturing should be added after the fractures are fully expanded, and the amount of pre-fluid should be increased to prevent sand from plugging in tortuous fractures.
(4) The stress-sensitive effect of natural fractures impacts the permeability of natural fractures and the fracturing fluid leak-off in natural fractures. Natural fractures are easily crossed by hydraulic fractures when their permeability is small. When the difference between the horizontal principal stresses is more than 20 MPa, the spread of fracturing fluid in the natural fracture will be strongly inhibited, and only a part of the natural fracture area in the sample is stained. Therefore, enhancing the permeability of natural fractures with corrosion fracture filler can increase the complexity of the fracture network.

Author Contributions: Conceptualization, Z.H. and P.C.; methodology, W.J.; validation, Y.Y.; formal analysis, Y.L.; investigation, L.Z.; resources, H.W.; writing—original draft preparation, Y.S. writing—review and editing, Y.P. All authors have read and agreed to the published version of the manuscript.

Funding: This research was funded by the National Natural Science Foundation of China (No. 52204051 and U21B2071) and the Natural Science Foundation of Sichuan Province (No. 2022NSFSC0971).

Data Availability Statement: Not applicable.

Conflicts of Interest: The authors declare no conflict of interest.

References

1. Khormali, A.; Petrakov, D.G.; Farmanzade, A.R. Prediction and Inhibition of Inorganic Salt Formation under Static and Dynamic Conditions—Effect of Pressure, Temperature, and Mixing Ratio. *Int. J. Technol.* **2016**, *7*, 943–951. [CrossRef]
2. Peng, Y.; Zhao, J.; Sepehrnoori, K.; Li, Z.; Xu, F. Study of delayed creep fracture initiation and propagation based on semi-analytical fractional model. *Appl. Math. Model.* **2019**, *72*, 700–715. [CrossRef]
3. Li, Y.; Luo, A.; Chen, X.; Cheng, L.; Chang, C.; Xie, W. A Novel model for simulating the integration process of hydraulic fracturing, shut-in period, and well production. *Front. Energy Res.* **2022**, *10*, 979526. [CrossRef]
4. Zhang, X.; Zhang, J.; Xiao, C. Experimental Investigation of Seepage Mechanism on Oil-Water Two-Phase Displacement in Fractured Tight Reservoir. *Geofluids* **2022**, *2022*, 6792154. [CrossRef]

5. Luo, A.; Li, Y.; Wu, L.; Peng, Y.; Tang, W. Fractured horizontal well productivity model for shale gas considering stress sensitivity, hydraulic fracture azimuth, and interference between fractures. *Nat. Gas Ind. B* **2021**, *8*, 278–286. [CrossRef]
6. Zhai, M.; Wang, D.; Li, L.; Zhang, Z.; Zhang, L.; Huang, B.; Li, A.; Zhang, Q. Investigation on the mechanism of hydraulic fracture propagation and fracture geometry control in tight heterogeneous glutenites. *Energy Explor. Exploit.* **2021**, *40*, 246–278. [CrossRef]
7. Xu, W.; Zhao, J.; Rahman, S.S.; Li, Y.; Yuan, Y. A Comprehensive Model of a Hydraulic Fracture Interacting with a Natural Fracture: Analytical and Numerical Solution. *Rock Mech. Rock Eng.* **2018**, *52*, 1095–1113. [CrossRef]
8. Chen, Z.; Liao, X.; Yu, W. A semianalytical well-testing model of fracture-network horizontal wells in unconventional reservoirs with multiple discretely natural fractures. *Nat. Gas Ind. B* **2020**, *7*, 567–582. [CrossRef]
9. Zhao, J.; Li, Y.; Wang, S.; Jiang, Y.; Zhang, L. Simulation of complex fracture networks influenced by natural fractures in shale gas reservoir. *Nat. Gas Ind. B* **2014**, *1*, 89–95.
10. Guo, J.; Lu, Q.; He, Y. Key issues and explorations in shale gas fracturing. *Nat. Gas Ind. B* **2023**, *10*, 183–197. [CrossRef]
11. Lamont, N.; Jessen, F.W. The effects of existing fractures in rocks on the extension of hydraulic fractures. *J. Pet. Technol.* **1963**, *15*, 203–209. [CrossRef]
12. Daneshy, A.A. Hydraulic fracture propagation in the presence of planes of weakness. In *SPE European Spring Meeting*; OnePetro: Richardson, TX, USA, 1974.
13. Warpinski, N.R.; Teufel, L.W. Influence of Geologic Discontinuities on Hydraulic Fracture Propagation. *J. Pet. Technol.* **1987**, *39*, 209–220. [CrossRef]
14. Blanton, T.L. Propagation of hydraulically and dynamically induced fractures in naturally fractured reservoirs. In *SPE Unconventional Gas Technology Symposium*; OnePetro: Richardson, TX, USA, 1986.
15. Blanton, T.L. An experimental study of interaction between hydraulically induced and pre-existing fractures. In *SPE Unconventional Gas Recovery Symposium*; OnePetro: Richardson, TX, USA, 1982.
16. Zhou, J.; Chen, M.; Jin, Y.; Zhang, G.-Q. Analysis of fracture propagation behavior and fracture geometry using a tri-axial fracturing system in naturally fractured reservoirs. *Int. J. Rock Mech. Min. Sci.* **2008**, *45*, 1143–1152. [CrossRef]
17. Renshaw, C.; Pollard, D. An experimentally verified criterion for propagation across unbounded frictional interfaces in brittle, linear elastic materials. *Int. J. Rock Mech. Min. Sci. Geomech. Abstr.* **1995**, *32*, 237–249. [CrossRef]
18. Zhou, J.; Jin, Y.; Chen, M. Experimental investigation of hydraulic fracturing in random naturally fractured blocks. *Int. J. Rock Mech. Min. Sci.* **2010**, *47*, 1193–1199. [CrossRef]
19. Gu, H.; Weng, X.; Lund, J.; Mack, M.; Ganguly, U.; Suarez-Rivera, R. Hydraulic Fracture Crossing Natural Fracture at Nonorthogonal Angles: A Criterion and Its Validation. *SPE Prod. Oper.* **2012**, *27*, 20–26. [CrossRef]
20. Gong, T.; Xia, B.; Liu, L.; Peng, Z.; Gao, Y. Propagation of hydraulic fracture under the joint impact of bedding planes and natural fractures in shale reservoirs. *Energy Sci. Eng.* **2019**, *7*, 2690–2702. [CrossRef]
21. Fatahi, H.; Hossain, M.; Sarmadivaleh, M. Numerical and experimental investigation of the interaction of natural and propagated hydraulic fracture. *J. Nat. Gas Sci. Eng.* **2017**, *37*, 409–424. [CrossRef]
22. Ai, C.; Li, X.-X.; Zhang, J.; Jia, D.; Tan, W.-J. Experimental investigation of propagation mechanisms and fracture morphology for coalbed methane reservoirs. *Pet. Sci.* **2018**, *15*, 815–829. [CrossRef]
23. Jiang, T.; Zhang, J.; Wu, H. Experimental and numerical study on hydraulic fracture propagation in coalbed methane reservoir. *J. Nat. Gas Sci. Eng.* **2016**, *35*, 455–467. [CrossRef]
24. Zou, Y.; Zhang, S.; Zhou, T.; Zhou, X.; Guo, T. Experimental Investigation into Hydraulic Fracture Network Propagation in Gas Shales Using CT Scanning Technology. *Rock Mech. Rock Eng.* **2016**, *49*, 33–45.
25. Hu, L.; Ghassemi, A. Laboratory-Scale Investigation of the Slippage of a Natural Fracture Resulting from an Approaching Hydraulic Fracture. *Rock Mech. Rock Eng.* **2021**, *54*, 2547–2558. [CrossRef]
26. Shi, Z.; Chen, J.; Gong, D.; He, S.; Jiang, X.; Sun, C.; Fan, L. Experimental study on the shear-slip characteristics of natural fractures in shale reservoirs. *Energy Sci. Eng.* **2022**, *10*, 1240–1250. [CrossRef]
27. Zhang, J.; Yu, Q.; Li, Y.; Pan, Z.; Liu, B. Hydraulic Fracture Vertical Propagation Mechanism in Interlayered Brittle Shale Formations: An Experimental Investigation. *Rock Mech. Rock Eng.* **2023**, *56*, 199–220. [CrossRef]
28. Dehghan, A.N. An experimental investigation into the influence of pre-existing natural fracture on the behavior and length of propagating hydraulic fracture. *Eng. Fract. Mech.* **2020**, *240*, 107330. [CrossRef]
29. Zhang, X.; Yin, M. Investigation of the Hydraulic Fracture Propagation Law of Layered Rock Strata Using the Discrete-Particle model. *Geofluids* **2022**, *2022*, 8038085. [CrossRef]
30. Kolawole, O.; Ispas, I. Interaction between hydraulic fractures and natural fractures: Current status and prospective directions. *J. Pet. Explor. Prod. Technol.* **2020**, *10*, 1613–1634. [CrossRef]
31. Kang, Y.; Hao, Z.; Chen, Q.; You, L.; Chen, M.; Tian, J.; Li, B. Heating-Induced Enhancement of Shale Gas Transport and Its Application for Improving Hydraulic Fracturing Performance. *Energy Fuels* **2022**, *36*, 14682–14695. [CrossRef]
32. Xia, Y.; Tan, P.; Wang, X.; Ren, L. Differences of fracture propagation behavior for two typical fractured formations. *Nat. Gas Ind. B* **2022**, *9*, 264–270. [CrossRef]
33. Chang, X. Laboratory analysis of liquid injection method on hydraulic fracturing initiation and propagation in deep shale formation. *Nat. Gas Ind. B* **2019**, *6*, 652–658. [CrossRef]
34. Daneshy, A. Three-Dimensional Analysis of Interactions Between Hydraulic and Natural Fractures. In *The SPE Hydraulic Fracturing Technology Conference and Exhibition*; OnePetro: Richardson, TX, USA, 2019.

35. He, Q.; Suorineni, F.; Oh, J. Modeling Interaction between Natural Fractures and Hydraulic Fractures in Block Cave Mining. In *The 49th U.S. Rock Mechanics/Geomechanics Symposium*; OnePetro: Richardson, TX, USA, 2015.
36. Chen, Q.; Hu, H.; Kang, Y.; You, L.; Zhou, Y.; Cheng, Q.; Liang, Y. Mitigating water blockage in shale matrix by acidizing or oxidizing treatment: Evidence from transport pathway change and diffusivity enhancement. *J. Pet. Sci. Eng.* **2022**, *219*, 111132. [CrossRef]